

Damping updating of a building structure installed with an MR damper

Sung-Sik Woo and Sang-Hyun Lee*

Department of Architectural Engineering, Dankook University, 126, Yongin-city, Korea

(Received November 20, 2012, Revised June 28, 2013, Accepted October 16, 2013)

Abstract. The purpose of this paper is to identify through experiments the finite element (FE) model of a building structure using a magnetorheological (MR) fluid damper. The FE model based system identification (FEBSI) technique evaluates the control performance of an MR damper that has nonlinear characteristics as equivalent linear properties such as mass, stiffness, and damping. The Bingham and Bouc-Wen models were used for modeling the MR damper and the equivalent damping increased by the MR damper was predicted by applying an equivalent linearization technique. Experimental results indicate that the predicted equivalent damping matches well with the experimentally obtained damping.

Keywords: damping updating; system identification; equivalent linearization; MR damper

1. Introduction

The magnetorheological (MR) fluid damper has either nonlinear force-displacement or a force-velocity relationship and its applicability to the control of civil structures has been investigated by many researchers (Dyke *et al.* 1996). Unlike linear damping devices, the control performance of nonlinear damping devices such as MR dampers is strongly dependent on the frequency and magnitude of the excitation load. Accordingly, the dynamic characteristics of the controlled structure and excitation load should be considered in the design of MR dampers (Jansen and Dyke 2000). If such nonlinear properties of the MR damper could be replaced by the equivalent linear system, the design procedure would be simplified and the amount of time required could be significantly reduced. Extensive researches have been conducted on an equivalent linear system to replace the nonlinear system. For a nonlinear hysteretic system excited by random signal, Caughey (1960) developed an equivalent system minimizing the root mean square of error and closely examined the characteristic of response with Gaussian distribution. Li and Reinhorn (1995) obtained the transfer function of a structure with a friction damper, and then expressed the effects of the friction damper as increased stiffness and damping matrices. Soong (1997) expressed the effect of the tuned mass damper as the increase of structural damping, and Yalla (2001) replaced the nonlinear damping coefficient of the tuned liquid column damper for an equivalent linear damping coefficient, which is obtained using an iteration procedure. Chang *et al.* (1993) proposed the equivalent damping ratio of a structure with viscous elastic dampers using the

*Corresponding author, Associate Professor, E-mail: lshyun00@dankook.ac.kr

modal strain energy method. Lee *et al.* (2004) presented a general method for evaluating the equivalent damping ratio of a system with nonlinear damping devices as well as linear damping devices. Chopra (2005) showed that the equivalent viscous damping can model the steady-state harmonic response of a system with Coulomb friction.

The purpose of this paper is to identify through experiments the finite element (FE) model of a building structure with an MR fluid damper. While general system identification methods provide system matrices which merely duplicate the input-output relationship but have no physical meanings, the FE model based system identification (FEBSI) technique estimates the mass, stiffness, and damping matrices of a structure (Friswell and Mottershead 1995). The force-displacement relationship of a practical MR damper is nonlinear and is generally described using the Bingham or Bouc-Wen model (Yang 2001). In this study, the equivalent damping coefficient of an MR damper was predicted by applying an equivalent linearization technique, and the value was compared with the experimentally obtained value from shaking table tests. The FE model of an uncontrolled system was first constructed using modal information for the natural frequency, damping ratio, and mode shape; the increased damping by the MR damper was then obtained by updating the damping matrix of the uncontrolled system to adjust the first modal damping ratio.

2. Equivalent linearization technique

2.1 Equivalent linear system

A nonlinear system can be substituted for an equivalent linear system as follows.

$$g(x, \dot{x}) = l_o + k_{eq}x + c_{eq}\dot{x} \quad (1)$$

where $g(x, \dot{x})$ denotes the non-linear system and l_o , k_{eq} , and c_{eq} are the mean component, equivalent stiffness, and equivalent damping, respectively. x and \dot{x} denote the displacement and velocity, respectively. The error between the non-linear and equivalent linear systems is generally defined as follows in terms of the mean square and the values of l_o , k_{eq} , and c_{eq} are determined to minimize this error.

$$\varepsilon = \lim_{T \rightarrow \infty} \frac{1}{T} \int_0^T \{g(x, \dot{x}) - l_o - k_{eq}x - c_{eq}\dot{x}\}^2 dt \quad (2)$$

where the response has Gaussian distribution, l_o , k_{eq} , and c_{eq} are given as

$$l_o = \int_{-\infty}^{\infty} g(x, \dot{x}) p(x) dx \quad (3)$$

$$k_{eq} = \frac{1}{\sigma_x^2} \int_{-\infty}^{\infty} g(x, \dot{x}) x p(x) dx \quad (4)$$

$$c_{eq} = \frac{1}{\sigma_{\dot{x}}^2} \int_{-\infty}^{\infty} g(x, \dot{x}) \dot{x} p(\dot{x}) d\dot{x} \quad (5)$$

where σ_x is the standard deviation of x and denotes the Gaussian probability density function

defined as

$$p(x) = \frac{1}{\sigma_x \sqrt{2\pi}} \exp\left(-\frac{x^2}{2\sigma_x^2}\right) \quad (6)$$

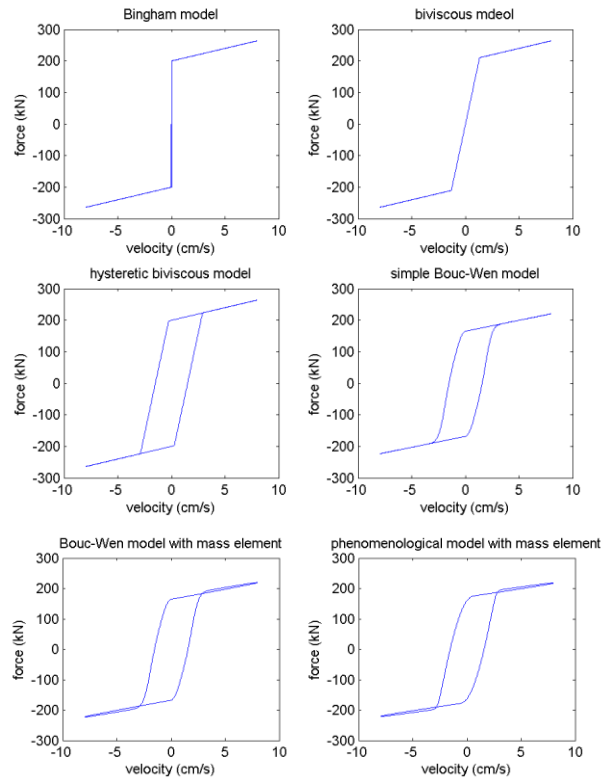


Fig. 1 Force-velocity relationship of 6 models for MR damper

2.2 Model for MR damper and equivalent linearization

Many models such as Bingham, biviscous, hysteretic biviscous, simple Bouc-Wen, Bouc-Wen with mass element, and phenomenon models have been developed for capturing the force characteristics of the MR dampers (Stanway *et al.* 1987, Gamota and Filisko 1991, Wereley *et al.* 1998, Bouc and Wen 1976, Spencer *et al.* 1997).

Yang (2001) presented the parameters for the dynamic models of the large scale 200 kN MR dampers. In this section, the analyses results obtained by using these models are compared for a three-story building structure. Fig. 1 shows the MR damper force-velocity relationship obtained by using the dynamic models used by Yang (2001) under a 1 inch, 0.5 Hz sinusoidal displacement excitation with an input current of 2 A. The hysteretic characteristics of the 6 models are different from each other, but the maximum values of the damping force are almost equivalent. Particularly, Bingham and biviscous models have a disadvantage: they cannot describe the hysteretic behavior.

Fig. 2 shows the time histories of the third floor displacement and absolute acceleration responses of the three story building structure with the MR damper at the first floor, and the peak values of inter-story displacement. The absolute accelerations are listed in Table 1. The considered building structure has identical story properties for all stories. Story mass, stiffness, and damping are, respectively, 100 metric ton, 98000 kN/m, and 140.7 kN·sec/m, and the El Centro (1942, NS component) earthquake is used as the input load. Fig. 2 and Table 1 show that the structural responses are significantly reduced by the use of the MR damper. However, the fact that the difference between the controlled structural responses of each model cannot be identified in Fig. 2 indicates that the essential parameter is not the shape of hysteretic curve but the magnitude of maximum control force. Accordingly, in this study whose purpose is not to accurately model of the MR damper, but to express the performance of the MR damper as equivalent linear properties such as stiffness and damping, the Bingham model and simple Bouc-Wen model are considered from hence.

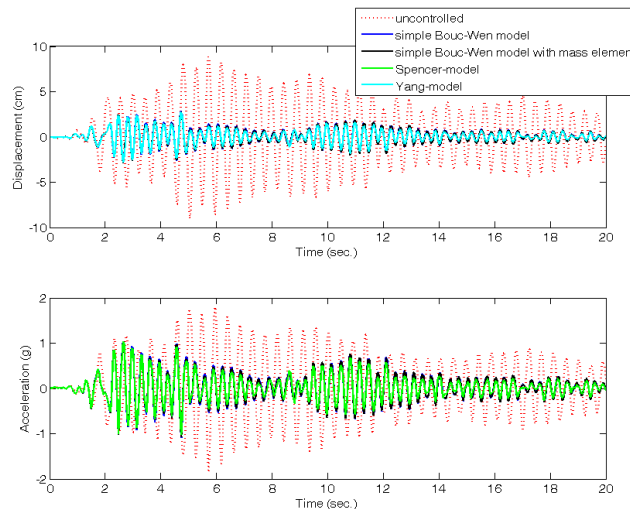


Fig. 2 Time histories of displacement and acceleration responses of the 3 story building

Table 1 Peak responses of 3 story building

	Floor	No Control	(1)	(2)	(3)	(4)	(5)	(6)
Max. Inter-story Disp. (cm)	1	4.2	1.8	1.8	1.8	1.6	1.7	1.7
	2	3.2	1.5	1.5	1.5	1.4	1.4	1.5
	3	1.9	0.9	0.9	0.8	0.8	0.8	0.8
Max. Acc. (cm/s ²)	1	975	461	468	495	461	499	522
	2	1477	672	662	665	618	649	661
	3	1814	880	872	831	769	806	811

(1) Bingham (2) biviscous (3) hysteretic biviscous (4) simple Bouc-Wen

(5) simple Bouc-Wen with mass element (6) phenomenological model

The Bingham model is given as a sum of coulomb friction and linear damping forces

$$F_1 = f_c \operatorname{sgn}(\dot{x}) + c\dot{x} \quad (7)$$

where f_c and c are the maximum friction force and damping coefficient, respectively, and $\operatorname{sgn}(\cdot)$ is a sign function.

Since Eq. (7) only has correlation with velocity, the equivalent stiffness is zero and only equivalent damping exists. Equivalent damping can be obtained using Eq. (5) when the response has Gaussian distribution.

$$c_{eq} = \sqrt{\frac{2}{\pi}} \frac{1}{\sigma_{\dot{x}}} f_c + c \quad (8)$$

The hysteresis of the MR damper can also be modeled using the Bouc-Wen Model.

$$F_2 = \alpha z + c\dot{x} + kx \quad (9)$$

where k and c are, respectively, the stiffness and the damping, and z is the non-dimensional variable used to describe the hysteresis of the MR damper. α is a variable depending on the input current to the MR damper. The variable z is governed by the following nonlinear differential equation.

$$\dot{z} = -\gamma|\dot{x}|z|z|^{n-1} - \beta\dot{x}|z|^n + A\dot{x} \quad (10)$$

where γ , β , A , and n are the parameters determining the shape of the hysteretic curve. Fig. 3 shows the z -displacement and z -velocity relationships in terms of various n and A for the system with $\gamma=0.5$ and $\beta=0.5$. Harmonic displacement with unit radial frequency and unit maximum magnitude is given. Figure 4 shows the corresponding equivalent stiffness and damping.

Figs. 3(a) and 3(d) with $A=1$ indicate that z is almost equal to the displacement, as presented in Fig. 4, showing that only equivalent stiffness exists and equivalent damping is close to zero when $A=1$. Figs. 3(a)-3(c) show that the positive correlation of z with displacement gradually decreases with increasing A , and this phenomenon is also presented in Fig. 4 by the decrease of equivalent stiffness with increasing A , except for $n=3$. The reason why equivalent stiffness increases for $n=3$ is not that the positive correlation of z with displacement increases, but simply that the magnitude of z increases with increasing A for $n=3$. Also, the increase of n reduces the equivalent stiffness and damping, which results not from any variation in the form of a hysteretic curve, but also from the increase of magnitude of z with increasing n . In other words, this phenomenon is a type of scale problem which is governed by the relative magnitudes of γ , β , and A .

The trends shown in Figs. 3 and 4 indicate that various types of nonlinear hysteretic curves can be modeled using the Bouc-Wen model and they can be expressed as equivalent linear stiffness and damping. The parameters of the Bouc-Wen model used for describing the MR damper are generally determined for z to show similar behavior to that shown in Fig. 3(c) (Yang 2001). If stiffness in an MR damper occurs, the stiffness is modeled simply by using linear stiffness as indicated by Eq. (9) rather than by using a Bouc-Wen model of which z shows similar behavior to that of Fig. 3(a). Consequently, the variable z of the Bouc-Wen model used for describing the hysteresis behavior of the MR damper plays a part in increasing equivalent damping.

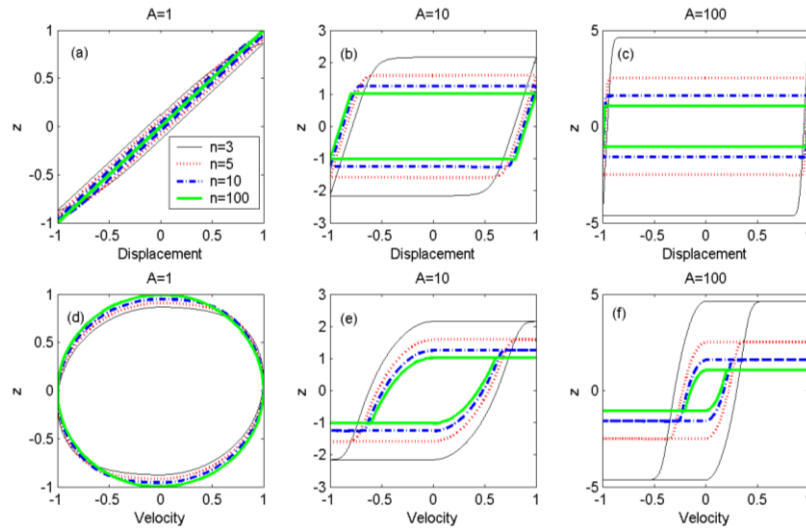


Fig. 3 \dot{z} -displacement and \dot{z} -velocity relationships ($\gamma=0.5$, $\beta=0.5$)

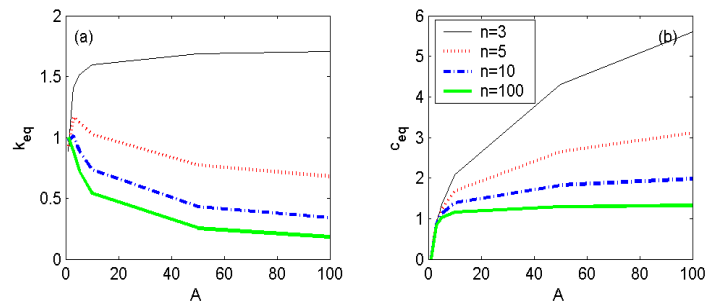


Fig. 4 Equivalent stiffness and damping ($\gamma=0.5$, $\beta=0.5$)

3. Experimental setup

3.1 Structure and measurement system

The experimental test using a shaking table was conducted in the Dynamics Laboratory at Dankook University, Seoul, Korea. A three-story and single-bay steel frame was used, as shown in Fig. 5. Since it was assumed that the masses are concentrated at each floor, the diagonal mass matrix could be constructed by directly measuring the mass of the each floor. The diagonal elements of the mass matrix are in regular sequence 26.24 kg, 26.24 kg and 23.12 kg. The height of the structure is 155 cm and the plan size is 60cm×60cm. Stiffness and damping matrices of uncontrolled structure shown in Fig. 3 can be constructed using the mass matrix, mass normalized eigenvector and eigenvalue matrices obtained by white noise excitation test (Hwang *et al.* 2005).

The accelerometers were positioned on each floor to measure the lateral absolute accelerations of the floor. The data acquisition was performed using a real-time digital signal processor (DSP)

with sampling frequency 100 Hz.



Fig. 5 Shaking table and 3 storey building model

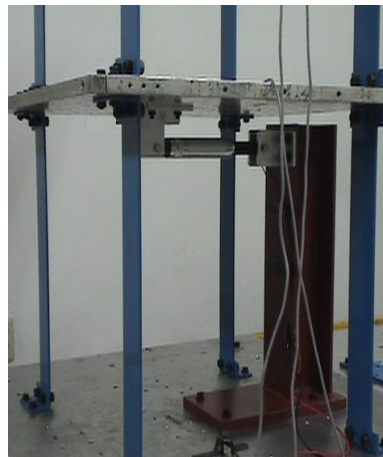


Fig. 6 MR damper implementation

3.2 MR damper installation

An MR damper RD-1097-01 manufactured by Lord Corporation is installed at the first floor of the structure. Fig. 6 shows the time history of the force generated by MR damper, force-displacement curve, and force-velocity curve obtained under the 1.5 Hz harmonic excitation (Lee *et al.* 2007). The parameters of Bingham model which best describe the behavior of the used MR damper are $C_o=10\text{N}\cdot\text{s/m}$ for all currents and $f_c=8\text{ N}$, 11.5 N, 20 N, 30 N, and 39 N for 0 A, 0.1 A, 0.2 A, 0.3 A, and 0.4 A, respectively. It is observed that the MR damper shows similar behavior to that of a friction damper and its maximum friction force varies from 8 N to 39 N according to the applied input current. The relative displacement of the first floor to the base is transferred to the MR damper, of which the ends are connected to an H-section column rigidly mounted on the base and jig fixed to the first floor.

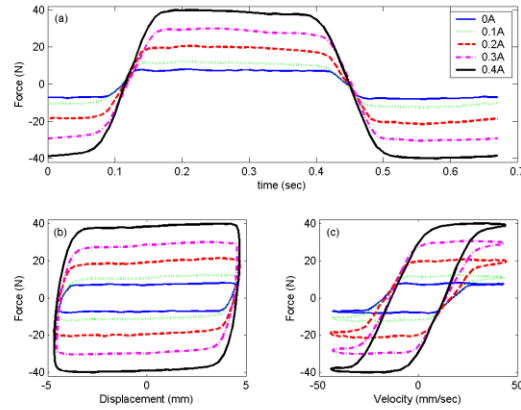


Fig. 7 Force of MR damper; (a) time-history, (b) force-displacement curve and (c) force-velocity curve (1.5 Hz) (Lee *et al.* 2007)

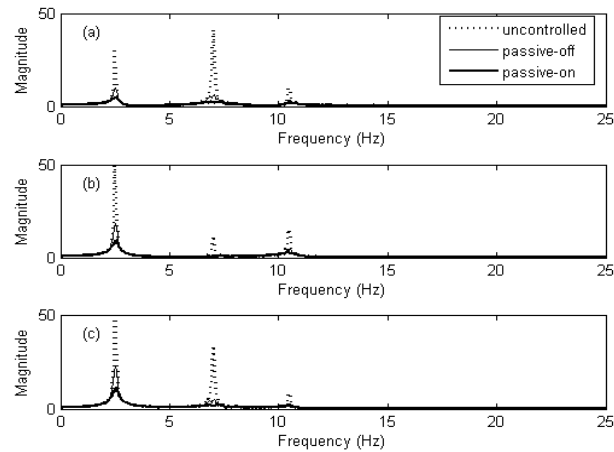


Fig. 8 Transfer function from base acceleration to floor acceleration: (a) 1st floor, (b) 2nd floor and (c) 3rd floor

4. Finite element based system identification

System identification is used to construct the system matrix which can describe the relationship between input and output exactly. By applying this system identification technique to a structure with a damper, the effect of the damper on the structure can be quantitatively evaluated. In this study, the equivalent stiffness and damping increased due to the MR damper are experimentally obtained by using the modal information on a 3-story building structure installed with an MR damper. Low-pass filtered white noise, of which the cut-off frequency is 25 Hz, is used as an input signal. The data was measured at a sampling time of 0.01 seconds for 100 seconds. Various control algorithms such as modified bang-bang, clipped optimal and sliding mode control have been used

for maximizing the performance of the MR damper (Jansen and Dyke 2000).

In previous study by Lee *et al.* (2011), the performance of the passive-on MR dampers on reducing displacement response was compared with the other semi-active MR dampers. When the maximum force of the MR damper was less than 30% of the maximum base shear force, the passive-on MR damper can show almost equivalent performance to the semi-active MR dampers. Therefore, in this study, only passive-on state was considered.

Fig. 8 plots the transfer function from the base acceleration to the absolute acceleration of each floor. Passive-off and passive-on are cases in which the input currents to the MR damper are 0A and 0.1 A, respectively. It is observed that the MR damper reduces the acceleration response of the building structure and the passive-on state is observed to be the most effective control performance. Also, Fig. 8 indicates that the first, second, and third modes definitely exist for uncontrolled and passive-off systems, while the second modal response of the passive-on system is significantly reduced. If the information on mode shape, frequency, and damping ratio of all modes is available, stiffness and damping matrices can be obtained. In this study, the modal information is obtained using the curve-fitting of the transfer function used by Li and Reinhorn (1995) for the system identification of a building structure with a friction damper; stiffness and damping matrices are then constructed as follows. It is assumed that the mass matrix is previously known and the mode vector is mass-normalized.

$$K = M\Phi\Omega\Phi^T M \quad (11)$$

$$C = M\Phi\Lambda\Phi^T M \quad (12)$$

where M is the mass matrix and Φ is the mass-normalized mode vector. Λ and Ω are

$$\Omega = \Phi^T K \Phi = \text{diag}(\omega_{ni}^2, i=1, \dots, n) \quad (13)$$

$$\Lambda = \Phi^T C \Phi = \text{diag}(2\xi_{ni}\omega_{ni}, i=1, \dots, n) \quad (14)$$

where ω_{ni} and ξ_i are the natural frequency and damping ratio of the i th mode, respectively.

The natural frequencies of the uncontrolled system are 2.48 Hz, 7.00 Hz, and 10.48 Hz, and the modal damping ratios are 0.94%, 0.32%, and 0.45%, respectively. By using Eqs. (11)-(14), the stiffness and damping matrices of the uncontrolled system are obtained as follows

$$K = \begin{bmatrix} 58.231 & -33.222 & -2.357 \\ -33.222 & 68.856 & -40778 \\ -2.357 & -40778 & 43815 \end{bmatrix} \text{ kN/m}, C = \begin{bmatrix} 9.0227 & -3.0468 & 1.7258 \\ -3.0468 & 11.8465 & -2.6404 \\ 1.7258 & -2.6404 & 9.8111 \end{bmatrix} \text{ N}\cdot\text{sec/m} \quad (15)$$

Since the MR damper renders the higher modes of the structure indistinct and increases the structural damping significantly, it is difficult to identify the stiffness and damping matrices of the structure with the MR damper using Eqs. (11) and (12). Also, this distributes the effects of the MR damper over all elements of the damping matrix. In the experiment of a three story building, the MR damper was installed only at the first floor. In order to clarify the physical meaning of the damper location, only the element (1,1) of the damping matrix of the uncontrolled system was updated because only c_1 is directly correlated with the first floor response. In this case, just one damping ratio from a specific mode should be used and the first modal damping ratio was chosen in this study. Damping matrix C should provide the same first modal damping ratio as the experimentally obtained ξ_{n1} .

$$f(c_1) = \frac{1}{2\omega_{n1}} \phi_1^T C \phi_1 - \xi_{n1} = 0 \quad (16)$$

in which ϕ_1 is the mass-normalized first modal vector and c_1 is the (1,1) element of C . The variation of c_1 satisfying Eq. (16) above is given as follows.

$$\Delta c_1 = - \left(\frac{\partial f(c_1)}{\partial c_1} \right)^{-1} f(c_1) = - \left(\frac{1}{2\omega_{n1}} \phi_1^T \frac{\partial C}{\partial c_1} \phi_1 \right)^{-1} f(c_1) \quad (17)$$

Table 2 shows the comparison between c_{eq} from Eq. (8) and Δc_1 from Eq. (17). Eq. (8) is used because the MR damper used shows similar behavior to that of the friction damper, which can be modeled by the Bingham model. The first modal damping ratios of the structure with a passive-off and passive-on MR damper are 2.67% and 5.44%, respectively. The value of $\sigma_{\dot{x}}$ in Eq. (8) is estimated using the measured acceleration response.

$$\sigma_{\dot{x}} = \sigma_{\ddot{x}} / \omega_{n1} \quad (18)$$

It is observed from Table 2 that the error between the predicted and experimentally obtained equivalent damping is less than 5%. This verifies that the equivalent linear damping can evaluate the performance of the MR damper and it can also be predicted by the equivalent linearization technique. The simple Bingham model provides little error because the magnitude of maximum friction force, which is the most important factor in determining the equivalent damping, can be accurately expressed by the Bingham model.

Table 2 Equivalent damping of the structure with MR damper

	c_{eq} (N·s/m)	Δc_1 (N·s/m)	Error(%) $100 \times (c_{eq} / \Delta c_1 - 1)$
Passive-off	138.9	132.9	4.6
Passive-on	333.7	342.2	-2.5

5. Conclusions

In this study, the performance of an MR damper having nonlinear characteristics was identified as an equivalent linear system. The stiffness and damping matrices of a three story building structure were formed using the data from a shaking table test; the damping matrix was then updated to adjust the first modal damping ratio increased by the MR damper. Equivalent damping of the MR damper described by the Bingham model was obtained by applying an equivalent linearization technique. Experimental results indicate that an equivalent linearization technique using the Bingham model can be used for predicting the effects of an MR damper as increased damping.

Acknowledgements

This research was supported by the research fund of Dankook University in 2011.

References

- Caughy, T.K. (1960), "Random excitation of a system with bilinear hysteresis", *J. Appl. Mech. - T. ASME.*, **27**, 649-652.
- Chang, K.C., Lai, M.L., Soong, T.T., Hao D.S. and Yeh, Y.C. (1993), *Seismic behavior and design guidelines for steel frame structures with added viscoelastic dampers*, Technical Report NCEER-93-0009, National Center for Earthquake Engineering Research.
- Chopra, A.K. (2001), *Dynamics of structures: Theory and applications to earthquake engineering*, 2nd Ed., Prentice Hall, Upper Saddle River, NJ.
- Dyke, S.J., Spencer Jr., B.F., Sain, M.K. and Carlson, J.D. (1996), "Modeling and control of magnetorheological dampers for seismic response reduction", *Smart Mater. Struct.*, **5**, 565-575.
- Friswell, M.I. and Mottershead, J.E. (1995), *Finite element model updating in structural dynamics*, Kluwer Academic Publishers, Boston, London.
- Gamota, D.R. and Filisko, F.E. (1991), "Dynamic mechanical studies of electrorheological materials: moderate frequencies", *J. Rheology*, **35**(3), 399-425.
- Hwang, J.S., Min, K.W., Lee, S.H. and Kim, H. (2005), "Probabilistic approach for active control of structures: experimental verification", *Earthq. Eng. Struct.D.*, **34**(3), 207-225.
- Jansen, L.M. and Dyke, S.J. (2000), "Semi-active control strategies for MR dampers: comparative study", *J. Eng. Mech. - ASCE*, **126**(8), 795-803.
- Lee, S.H., Min, K.W., Kim, J.K. and Hwang, J.S. (2004), "Equivalent damping ratio of a structure with added dampers", *Eng. Struct.*, **26**(3), 335-346.
- Lee, S.H., Min, K.W., Chun, L., Lee, S.K., Lee, M.K., Hwang, J.S., Choi, S.B. and Lee, H.G. (2007), "Bracing system for installation of MR dampers in a building structure", *J. Intel. Mat. Syst. Str.*, **18**(11), 1111-1120.
- Lee, S.H., Yun, K.J. and Min, K.W. (2011), "A decentralized response-dependent MR damper for controlling building structures excited by seismic load", *J. Intel. Mat. Syst. Str.*, **22**(16), 1913-1927.
- Li, C. and Reinhorn, J.C. (1995), *Experimental and analytical investigation of seismic retrofit of structures with supplemental damping: part II-friction devices*, Technical Report NCEER-95-0009, National Center for Earthquake Engineering Research.
- Soong, T.T. and Dargush, G.F. (1997), *Passive energy dissipation systems in structural engineering*, John Wiley & Sons Ltd, Chichester, England.
- Spencer Jr., B.F., Dyke, S.J., Sain, M.K. and Carlson, J.D. (1997), "Phenomenological model for magnetorheological dampers", *J. Eng. Mech. - ASCE*, **123**(3), 230-238.
- Stanway, R., Sproston, J.L. and Stevens, N.G. (1987), "Non-linear modeling of an electro-rheological vibration damper", *J. Electrostatics*, **20**(2), 167-184.
- Wen, Y.K. (1976), "Method of random vibration of hysteretic systems", *J. Eng. Mech. - ASCE*, **102**(2), 249-263.
- Wereley, N.M., Pang, L. and Kamath, G.M. (1998), "Idealized hysteresis modeling of electrorheological and magnetorheological dampers", *J. Intel. Mat. Syst. Str.*, **9**(8), 642-649.
- Yalla, S.K. (2001), *Liquid dampers for mitigation of structural response: theoretical development and experimental validation*, Ph.D Dissertation, Univ. of Notre Dame,
- Yang, G. (2001), *Large-scale magnetorheological fluid damper for vibration mitigation: modeling, testing and Control*, Ph.D Dissertation, Univ. of Notre Dame.